Inorg. Chem. **2008**, *47*, 3709−3718

Reporting a New Class of Divanadium(V) Compounds Connected by an Unsupported Hydroxo Bridge

Pabitra Baran Chatterjee,[†] Debdas Mandal,[†] Anandalok Audhya,[†] Ki-Young Choi,[‡] Akira Endo,[||] and Muktimoy Chaudhury*,[†]

Department of Inorganic Chemistry, Indian Association for the Cultivation of Science, Kolkata 700 032, India, Department of Chemistry Education, Kongju National University, Kongju 314-701, South Korea, and Department of Chemistry, Faculty of Science and Technology, Sophia University, 7-1, Kioi-cho, Chiyoda-ku, Tokyo 102-8554, Japan

Received November 21, 2007

Dinuclear oxovanadium(V) compounds [$LV^{V}O(\mu$-OH)$OV^{V}L](PF_6)$ [H_2L = *N,N′*-tert-ethylene bis(salicylideneimine) (H_2Salen) and its derivatives] (**1**–**3**) have been obtained by aerial oxidation of $V^{IV}OL$ precursors in THF in the presence of added NH_4PF_6. The oxidized vanadium(V) probably extracts an OH^- ligand from the residual moisture in the solvent and is retained as an unsupported hydroxo-bridge between the metal centers of these compounds as confirmed by single-crystal X-ray diffraction analyses. The molecules of **1**–**3** have centrosymmetric structures with each vanadium center having a distorted octahedral geometry. The bridging OH^- group is located *trans* to the terminal $V{=}O_t$ bond. The latter exerts strong *trans* labilizing influence to set the participating vanadium centers apart by about 4.1 Å. These separations are by far the largest (e.g., V···V#, 4.131 Å in **1**) among all binuclear compounds containing an unsupported hydroxo bridge reported to date. The complexes retain their identity also in solution as established by ^{1}H NMR spectroscopy. Electrochemically, the behaviors of **1**–**3** are quite interesting as studied by cyclic voltammetry in acetonitrile, each undergoing three (except **3**) nearly reversible metal-based reductions, all in the positive potential range (e.g., at $E_{1/2}$ = 0.57, 0.39, and 0.04 V versus Ag/AgCl reference for **1**) as indicated by steady state voltammetry. The electrode process at 0.39 V appears to involve a single-step two-electron transfer as revealed from the normal and differential pulse voltammetric data and probably includes a combination of $V^{V}-V^{IV} \leftrightarrow V^{III}-V^{IV}$ mixed oxidation states. Compounds **1**–**3** thus provide a unique example of divanadium compounds in which the metal centers are linked by an unsupported hydroxo-bridge.

Introduction

Dinuclear metal complexes connected by a sole μ-oxo bridge continue to attract increasing attention in contemporary coordination chemistry. Such species, often supported by ancillary bridging ligand(s) (viz. carboxylates, etc.) are known to play pivotal roles in biology during dioxygen activation by a host of metalloenzymes, namely, methane monooxygenase, Δ^9-desaturase, ribonucleotide reductase, cytochrome *c* oxidase, and so forth.[1−3] These enzymes containing homo- ($Fe^{II/IV}$, $Fe^{II/IV}$) and heterobinuclear (Fe^{II}, Cu^{II}) active sites are known to activate dioxygen molecule by a variety of complex mechanisms which frequently involve a putative μ-hydroxo species as a key intermediate, responsible for the oxidation of organic substrates.[4] Efficient use of μ-oxo species as catalysts by mother nature in the biological domain is a source of motivation for chemists to replicate the use of such species as efficient catalysts.[5]

Unlike the single μ-oxo bridged binuclear complexes, the chemistry of "unsupported" μ-hydroxo bridged analogues is less explored because of the lack of any straightforward

* Author to whom correspondence should be addressed. E-mail: icmc@iacs.res.in.
† Indian Association for the Cultivation of Science.
‡ Kongju National University.
|| Sophia University.

(1) (a) Wallar, B. J.; Lipscomb, J. D. *Chem. Rev.* **1996**, *96*, 2625. (b) Solomon, E. I.; Brunold, T. C.; Davis, M. I.; Kemsley, J. N.; Lee, S. K.; Lehnert, N.; Neese, F.; Skulan, A. J.; Yang, Y.-S.; Zhou, J. *Chem. Rev.* **2000**, *100*, 235. (c) Tshuva, E. Y.; Lippard, S. J. *Chem. Rev.* **2004**, *104*, 987. (d) Que, L., Jr.; True, A. E. *Prog. Inorg. Chem.* **1990**, *38*, 97;. and references therein.
(2) Ferguson-Miller, S.; Babcock, G. T. *Chem. Rev.* **1996**, *96*, 2889.
(3) Kim, E.; Chufán, E. E.; Kamaraj, K.; Karlin, K. D. *Chem. Rev.* **2004**, *104*, 1077.

10.1021/ic702286h CCC: $40.75
Published on Web 04/11/2008

method for their synthesis. However, the relevance of such species as a model for many oxidase biosites has prompted several studies with the objective to synthesize "unsupported" μ-hydroxo binuclear compounds involving both homo and heterometal centers that helped in unfolding the chemistry associated with such complex biomolecules.[6–12]

In vanadium chemistry, the ubiquity of oxovanadium species in higher oxidation states (4+ and 5+) is well established. A large number of unsupported μ-oxo divanadium compounds containing $[V_2O_3]^{n+}$ ($n = 2$, 3, and 4) cores have been already reported and discussed briefly in our previous communications.[13] Far less numerous are the hydroxo-bridged divanadium compounds. Surprisingly, to our knowledge, all the μ-hydroxo divanadium compounds reported thus far[14–17] have one or more supporting bridging group(s) [B and X] that can be classified under the following four categories (Chart 1) depending upon the type and the number of supporting bridges. The results seem to suggest that a sole μ-OH bridge by itself is not capable of holding the vanadium centers together!

Chart 1. Classification of the Hydroxo-Bridged Divanadium Compounds Containing One or More Supporting Bridge(s) Found in μ-Hydroxo Divanadium Compounds

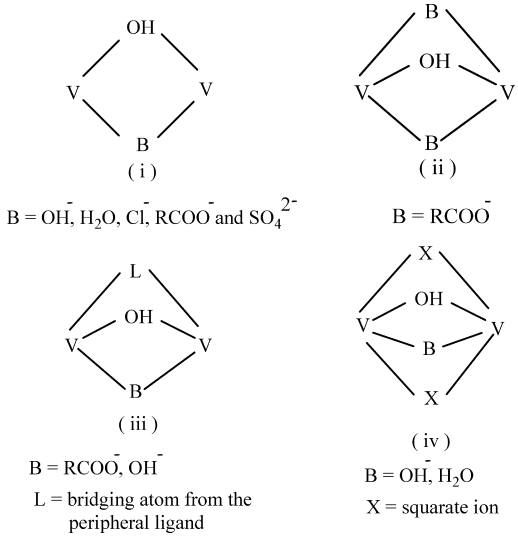

Herein, we report a new class of divanadium(V) compounds (**1**–**3**) containing a hitherto unknown $[V_2O_2(OH)]^{5+}$ core. Oxovanadium(V) centers in these compounds are connected by a single μ-OH group with no further ancillary bridging moiety. Results of single-crystal X-ray diffraction analysis, NMR spectroscopy (including ^{1}H, ^{19}F, and ^{51}V), and electrospray ionization mass spectra (ESI-MS) studies have confirmed such unprecedented bridging mode in **1**–**3** both in the solid state as well as in solution. Complete details on the preparation and structural and physicochemical properties of all the compounds (**1**–**3**) have been discussed.

Experimental Section

Materials. Unless stated otherwise, all reactions were carried out under an atmosphere of purified dinitrogen. Precursor complexes [VO(Salen)] and its analogues were prepared following the literature methods.[18] All other reagents are commercially available and used as received. Solvents were reagent grade, dried by standard methods,[19] and distilled under nitrogen prior to their use.

Preparation of Complexes. [(L^1)OV(μ-OH)VO(L^1)]PF_6·2THF (1).[20] To a stirred solution of [VO(Salen)] (0.17 g, 0.5 mmol) in tetrahydrofuran (THF, 25 mL) was added solid ammonium

(4) (a) DeRose, V. J.; Liu, K. E.; Kurtz, D. M., Jr.; Hoffman, B. M.; Lippard, S. J. *J. Am. Chem. Soc.* **1993**, *115*, 6440. (b) Liu, K. E.; Valentine, A. M.; Wang, D.; Huynh, B. H.; Edmondson, D. E.; Salifoglou, A.; Lippard, S. J. *J. Am. Chem. Soc.* **1995**, *117*, 10174. (c) Han, S.; Ching, Y.-C.; Rousseau, D. L. *Nature* **1990**, *348*, 89. ; and references therein.

(5) (a) Singh, S.; Roesky, H. W. *Dalton Trans.* **2007**, 1360. (b) Bottomley, F.; Goh, S.-K. *Polyhedron* **1996**, *15*, 3045.

(6) (a) Scheidt, W. R.; Cheng, B.; Safo, M. K.; Cukiernik, F.; Marchon, J.-C.; Debrunner, P. G. *J. Am. Chem. Soc.* **1992**, *114*, 4420. (b) Evans, D. R.; Mathur, R. S.; Heerwegh, K.; Reed, C. A.; Xie, Z. *Angew. Chem., Int. Ed. Engl.* **1997**, *36*, 1335. (c) Hung, C.-H.; Chen, W.-C.; Lee, G.-H.; Peng, S.-M. *Chem. Commun.* **2002**, 1516. (d) Armentano, D.; De Munno, G.; Mastropietro, T. F.; Julve, M.; Lloret, F. *J. Am. Chem. Soc.* **2005**, *127*, 10778. (e) Jullien, J.; Juhász, G.; Mialane, P.; Dumas, E.; Mayer, C. R.; Marrot, J.; Rivière, E.; Bominaar, E. L.; Munck, E.; Sécheresse, F. *Inorg. Chem.* **2006**, *45*, 6922.

(7) (a) Haddad, M. S.; Wilson, S. R.; Hodgson, D. J.; Hendrickson, D. N. *J. Am. Chem. Soc.* **1981**, *103*, 384. (b) Burk, P. L.; Osborn, J. A.; Youinou, M.-T.; Angus, Y.; Louis, R.; Weiss, R. *J. Am. Chem. Soc.* **1981**, *103*, 1273. (c) Harding, C. J.; Mckee, V.; Nelson, J.; Lu, Q. *J. Chem. Soc., Chem. Commun.* **1993**, 1768. (d) Koval, I. A.; van der Schilden, K.; Schuitema, A. M.; Gamez, P.; Belle, C.; Pierre, J.-L.; Luken, M.; Krebs, B.; Roubeau, O.; Reedijk, J. *Inorg. Chem.* **2005**, *44*, 4372.

(8) (a) Cheng, B.; Cukiernik, F.; Fries, P. H.; Marchon, J.-C.; Scheidt, W. R. *Inorg. Chem.* **1995**, *34*, 4627. (b) Cheng, B.; Fries, P. H.; Marchon, J.-C.; Scheidt, W. R. *Inorg. Chem.* **1996**, *35*, 1024.

(9) (a) Nanthakumar, A.; Fox, S.; Murthy, N. N.; Karlin, K. D. *J. Am. Chem. Soc.* **1993**, *115*, 8513. (b) Kopf, M.-A.; Neuhold, Y.-M.; Zuberbühler, A. D.; Karlin, K. D. *Inorg. Chem.* **1999**, *38*, 3093.

(10) Scott, M. J.; Zhang, H. H.; Lee, S. C.; Hedman, B.; Hodgson, K. O.; Holm, R. H. *J. Am. Chem. Soc.* **1995**, *117*, 568.

(11) Donzello, M. P.; Bartolino, L.; Ercolani, C.; Rizzoli, C. *Inorg. Chem.* **2006**, *45*, 6988.

(12) Chufán, E. E.; Verani, C. N.; Puiu, S. C.; Rentschler, E.; Schatzschneider, U.; Incarvito, C.; Rheingold, A. L.; Karlin, K. D. *Inorg. Chem.* **2007**, *46*, 3017.

(13) (a) Chatterjee, P. B.; Kundu, N.; Bhattacharya, S.; Choi, K.-Y.; Endo, A.; Chaudhury, M. *Inorg. Chem.* **2007**, *46*, 5483; and references therein. (b) Dutta, S. K.; Samanta, S.; Kumar, S. B.; Han, O. H.; Burckel, P.; Pinkerton, A. A.; Chaudhury, M. *Inorg. Chem.* **1999**, *38*, 1982. (c) Dutta, S. K.; Kumar, S. B.; Bhattacharyya, S.; Tiekink, E. R. T.; Chaudhury, M. *Inorg. Chem.* **1997**, *36*, 4954.

(14) (a) Wieghardt, K.; Bossek, U.; Volckmar, K.; Swiridoff, W.; Weiss, J. *Inorg. Chem.* **1984**, *23*, 1387. (b) Dean, N. S.; Bond, M. R.; O'Connor, C. J.; Carrano, C. J. *Inorg. Chem.* **1996**, *35*, 7643. (c) Kondo, M.; Ohrui, T.; Kawata, S.; Kitagawa, S. *Acta Crystallogr.: Cryst. Struct. Commun.* **1996**, *52C*, 2448. (d) Kosugi, M.; Hickichi, S.; Akita, M.; Moro-oka, Y. *Inorg. Chem.* **1999**, *38*, 2567. (e) Thiele, K.; Gorls, H.; Imhof, W.; Seidd, W. *Z. Anorg. Allg. Chem.* **1999**, *625*, 1927. (f) Cornman, C. R.; Geiser-Bush, K. M.; Kampf, J. W. *Inorg. Chem.* **1999**, *38*, 4303. (g) Paul, G.; Choudhury, A.; Nagarajan, R.; Rao, C. N. R. *Inorg. Chem.* **2003**, *42*, 2004. (h) Paine, T. K.; Weyhermüller, T.; Slep, L. D.; Neese, F.; Bill, E.; Bothe, E.; Wieghardt, K.; Chaudhuri, P. *Inorg. Chem.* **2004**, *43*, 7324.

(15) (a) Carrano, C. J.; Verastgue, R.; Bond, M. R. *Inorg. Chem.* **1993**, *32*, 3589. (b) Bond, M. R.; Czernuszewicz, R. S.; Dave, B. C.; Yan, Q.; Mohan, M.; Verastegue, R.; Carrano, C. J. *Inorg. Chem.* **1995**, *34*, 5857.

(16) (a) Müller, A.; Rohlfing, R.; Krickemeyer, E.; Bögge, H. *Angew. Chem., Int. Ed. Engl.* **1993**, *32*, 909. (b) Khan, M. I.; Chang, Y.-D.; Chen, Q.; Salta, J.; Lee, Y.-S.; O'Connor, C. J.; Zubieta, J. *Inorg. Chem.* **1994**, *33*, 6340. (c) Brouca-Cabarrecq, C.; Mohanu, A.; Millet, P.; Trombe, J. C. *J. Solid State Chem.* **2004**, *117*, 2575.

(17) (a) Neves, A.; Wieghardt, K.; Nuber, B.; Weiss, J. *Inorg. Chim. Acta* **1988**, *150*, 183. (b) Kanamori, K.; Okayasu, T.; Okamoto, K. *Chem. Lett.* **1995**, 105. (c) Kanamori, K.; Yamamoto, K.; Okayasu, T.; Matsui, N.; Okamoto, K.; Mori, W. *Bull. Chem. Soc. Jpn.* **1997**, *70*, 3031. (d) Tolis, E. J.; Manos, M. J.; Terzis, A.; Raptopoulou, C. P.; Kabanos, T. A. *J. Chem. Soc., Dalton Trans.* **2003**, 775.

(18) Bonadies, J. A.; Carrano, C. J. *J. Am. Chem. Soc.* **1986**, *108*, 4088.

(19) Perrin, D. D.; Armarego, W. L. F.; Perrin, D. R. *Purification of Laboratory Chemicals*, 2nd Ed.; Pergamon: Oxford, England, 1980.

hexafluorophosphate (0.16 g, 1.0 mmol) in portions. The resulting mixture was refluxed for about 3 h, when a green solution was obtained. It was then cooled and filtered. The filtrate volume was reduced to about 15 mL by rotary evaporation, allowed to stand in the air for about 24 h, and became gradually blue in color. The solution was finally cooled at 4 °C in a refrigerator for an overnight period. A brown crystalline compound deposited at this stage was collected by filtration, washed with diethyl ether (3 × 10 mL), and finally dried in vacuo over P_4O_{10}. Yield: 0.14 g (57%). Anal. Calcd for $C_{40}H_{45}N_4O_9V_2PF_6$: C, 49.35; H, 4.63; N, 5.76. Found: C, 48.96; H, 4.57; N, 5.69%. FT-IR bands (KBr pellet, cm^{-1}): 3438br, 1625s, 1598s, 1554s, 1446m, 1275s, 951s, 843vs, 816m, 760s, 658s, 557s, 462s. UV–vis (CH_3CN) [λ_{max}, nm (ε, mol^{-1} cm^2)]: 572 (2100); 325 (17200); 285 (sh); 249 (51650); 223 (65800). ^{51}V NMR (500 MHz, acetonitrile-d_3, 299 K, δ/ppm): −584 (s) [$\Delta\nu_{1/2}$, 2500 Hz]. ^{19}F NMR (500 MHz, acetonitrile-d_3, 299 K, δ/ppm): −72.27 (d, $J_{P—F}$ = 751 Hz, PF_6). Λ_M (CH_3CN/Ω^{-1} cm^2 mol^{-1}): 131. ESI-MS (positive) in CH_3CN: *m*/*z*, 684.14 $[M\text{-}PF_6\text{-}2THF]^+$.

$[(L^2)OV(\mu\text{-}OH)VO(L^2)]PF_6$ (2). This compound was prepared as a brown crystalline solid following essentially the same procedure as described for **1** using $[VO(L^2)]$ as the precursor complex. Yield: 0.13 g (61%). Anal. Calcd for $C_{34}H_{33}N_4O_7V_2PF_6$: C, 47.64; H, 3.85; N, 6.54. Found: C, 47.25; H, 3.76; N, 6.44%. FT-IR bands (KBr pellet, cm^{-1}): 3443br, 2926m, 1626s, 1599s, 1554m, 1446m, 1277s, 956s, 843vs, 816m, 750s, 656s, 559s, 459s. UV–vis (CH_3CN) [λ_{max}, nm (ε, mol^{-1} cm^2)]: 571 (2400); 332 (17500); 290 (sh); 252 (89000); 223 (116500). ^{51}V NMR (500 MHz, acetonitrile-d_3, 299 K, δ/ppm): −580 (s) [$\Delta\nu_{1/2}$, 3600 Hz]. ^{19}F NMR (500 MHz, acetonitrile-d_3, 299 K, δ/ppm): −72.27 (d, $J_{P—F}$ = 750.5 Hz, PF_6). Λ_M ($CH_3CN/\ \Omega^{-1}$ cm^2 mol^{-1}): 134. ESI-MS (positive) in CH_3CN: *m*/*z*, 711.70 $[M\text{-}PF_6]^+$.

$[(L^3)OV(\mu\text{-}OH)VO(L^3)]PF_6$ (3). An identical procedure as mentioned above (for **1**) yielded the product **3** in 37% yield when $[VOL^3]$ was employed as a replacement for [VO(Salen)]. Anal. Calcd for $C_{36}H_{37}N_4O_{11}V_2PF_6$: C, 45.50; H, 3.90; N, 5.90. Found: C, 45.17; H, 3.85; N, 5.81%. FT-IR bands (KBr pellet, cm^{-1}): 3428br, 2929m, 1628s, 1597m, 1563m, 1445s, 1269s, 1084s, 947s, 843vs, 815m, 737s, 652s, 559s, 462m. UV–vis (CH_3CN) [λ_{max}, nm (ε, mol^{-1} cm^2)]: 644 (2200); 352 (17100); 255 (60500). ^{51}V NMR (500 MHz, acetonitrile-d_3, 299 K, δ/ppm): −564 (s) [$\Delta\nu_{1/2}$, 3600 Hz]. ^{19}F NMR (500 MHz, acetonitrile-d_3, 299 K, δ/ppm): −72.30 (d, $J_{P—F}$ = 750.5 Hz, PF_6). Λ_M (CH_3CN/Ω^{-1} cm^2 mol^{-1}): 143. ESI-MS (positive) in CH_3CN: *m*/*z*, 803.89 $[M\text{-}PF_6]^+$.

Physical Measurements. Microanalyses (for C, H, and N) were performed at IACS on a Perkin-Elmer model 2400 Series II elemental analyzer. UV–visible spectral measurements in solution were recorded on a Perkin-Elmer model Lambda 950 UV–vis-NIR spectrophotometer, while for IR spectra, a Shimadzu model 8400S FT-IR spectrometer with samples prepared as KBr pellets was employed. ^1H NMR (300 MHz) spectra were recorded on a Bruker model Avance DPX 300 spectrometer using $SiMe_4$ (δ_0) as internal reference. ^{51}V and ^{19}F NMR spectra were obtained on a JEOL Lambda 500 spectrometer (500 MHz) with data analysis system (ALICE) operating at ambient temperature (299 K). Chemical shifts were referenced to external neat $VOCl_3$ and CF_3COOH, respectively. The ESI-MS in positive ion mode were measured on a Micromass Qtof YA 263 mass spectrometer. Molar conductivities (Λ_M) for a 1 mM solution of the complexes **1–3** in acetonitrile were measured at 298 K with a Systronics model 306 bridge.

Cyclic voltammetry in acetonitrile was recorded on a BAS model 100 B/W electrochemical workstation using a platinum disk (i.d. = 1.6 mm) working electrode and a platinum wire counter electrodes. Ag/AgCl was used for reference and Fc/Fc^+ couple as the internal standard. Solutions were ∼1.0 mM in the samples and contain 0.1 M TBAP as supporting electrolyte.

X-ray Crystallography. Crystals suitable for X-ray diffraction analyses were grown by slow evaporation from solutions in THF at 4 °C. Single crystals of **1** (plate, black crystals, 0.302 × 0.295 × 0.106 mm^3), **2** (block, black crystals, 0.186 × 0.100 × 0.071 mm^3), and **3** (rod like, black crystals, 0.177 × 0.089 × 0.082 mm^3) were mounted on glass fibers without protection. Cell dimensions were determined at 293 K from the setting angles of a Bruker SMART 1000 CCD diffractometer using a graphite monochromated Mo Kα (λ = 0.71073 Å) radiation source. Data collections were completed using the $\omega/2\theta$ scan techniques. There was no deterioration of the crystals during the data collections. Accurate cell dimensions were refined from setting angles of 5158, 2220, and 3629 reflections for **1**, **2**, and **3**, respectively, in the ranges of θ, 2.3005–26.5575° (**1**), 2.218–20.507° (**2**), and 2.219–23.4635° (**3**). Pertinent cell parameters, data collection conditions, and refinement details are provided in Table 1. The structures were solved by direct methods,[21] developed by successive difference Fourier synthesis and refined on F^2 by a full-matrix least-squares procedure using the SHELXL-97 program.[22] The positions of all nonhydrogen atoms were refined with anisotropic displacement factors. The hydrogen atoms except on the central bridging moiety (i.e., hydroxo-bridge) were geometrically calculated and isotropically fixed at positions recalculated after each cycle of refinement [d(C−H) = 0.95 Å, with the isotropic thermal parameter of $U_{iso}(H) = 1.2\ U_{iso}(C)$]. In all the cases, absorption corrections based on multiscan using *SADABS* (Sheldrick, 1996) software[23] were applied. The P atom of the hexafluorophosphate anion in **1** also lies on a crystallographic mirror plane. Data reduction was accomplished using the SAINT plus software,[24] and crystallographic diagrams were drawn using the (Oak Ridge thermal ellipsoid plot) ORTEP-3 at the 30% probability level.[25]

Results and Discussion

Syntheses. Unsupported hydroxo-bridged divanadium(V) compounds **1–3** have been prepared for the first time through a single-pot synthesis as outlined in Scheme 1. Quite a few vanadium compounds with a hydroxo group as ligand have been synthesized. Some of these compounds contain an OH group as a terminal ligand[14d,26] showing interesting relevance to metallobiosites.[26] In the majority of these compounds, however, it is attached in the μ-OH mode along with one or

(20) Abbreviations used: H_2L^1, *N*, *N*′-bis(salicylidene)-1,2-diaminoethane; H_2L^2, *N*, *N*′-bis(salicylidene)-1,2-diaminopropane; H_2L^3, *N*, *N*′-bis(3-methoxysalicylidene)-1,2-diaminoethane; TBAP, tetrabutylammonium perchlorate.

(21) Sheldrick, G. M. *Acta Crystallogr.* **1990**, *46A*, 467.
(22) Sheldrick, G. M. *SHELXL-97, Program for Crystal Structure Refinements*; University of Göttingen: Göttingen, Germany, 1996.
(23) Sheldrick, G. M. *SADABS, Program for Empirical Absorption Correction of Area Detector Data*; University of Göttingen: Göttingen, Germany, 1996.
(24) *SAINT-plus*, software users guide, Version 6.0; Bruker Analytical X-ray Systems: Madison, WI, 1999.
(25) Farrugia, L. J. *ORTEP-3 for WINDOWS*; University of Glasgow: Glasgow, Scotland, 1997.
(26) (a) Tolis, E. J.; Manos, M. J.; Tasiopoulos, A. J.; Raptopoulou, C. P.; Terzis, A.; Sigalas, M. P.; Deligiannakis, Y.; Kabanos, T. A. *Angew. Chem., Int. Ed.* **2002**, *41*, 2797. (b) Triantafillou, G. D.; Tolis, E. I.; Terzis, A.; Deligiannakis, Y.; Raptopoulou, C. P.; Sigalas, M. P.; Kabanos, T. A. *Inorg. Chem.* **2004**, *43*, 79. (c) Knopp, P.; Wieghardt, K.; Nuber, B; Weiss, J.; Sheldrick, W. S. *Inorg. Chem.* **1990**, *29*, 363. (d) Messerschmidt, A.; Wever, R. *Proc. Natl. Acad. Sci. U. S. A.* **1996**, *93*, 392.

Table 1. Summary of the Crystallographic Data for the Complexes **1**, **2**, and **3**

parameter	1	2	3
composition	$C_{40}H_{45}N_4O_9V_2PF_6$	$C_{34}H_{33}N_4O_7V_2PF_6$	$C_{36}H_{37}N_4O_{11}V_2PF_6$
fw	972.65	856.49	948.55
crystal system	monoclinic	triclinic	tetragonal
space group	$P2_1/c$	$P\bar{1}$	$I4_1/acd$
a, Å	13.3764(8)	9.8688(9)	24.9901(10)
b, Å	12.4181(8)	11.7361(10)	24.9901(10)
c, Å	12.6910(8)	17.0989(15)	27.0502(11)
α, deg	90.00	84.526(2)	90.00
β, deg	96.0200(10)	77.938(2)	90.00
γ, deg	90.00	75.156(2)	90.00
V, Å^3	2096.5(2)	1870.2(3)	16893.0(10)
ρ_{calc}, Mg m^{-3}	1.541	1.521	1.492
temp, K	293(2)	293(2)	293(2)
λ (Mo Kα), Å	0.71073	0.71073	0.71073
Z	2	2	16
$F(000)$, μ mm^{-1}	1000/0.570	872/0.624	7744/0.568
$2\theta_{max}$ [°]	56.70	56.66	56.58
reflections collected/unique	21182/5238	19233/9150	59632/5256
R_{int}, GOF on F^2	0.0343/1.051	0.0622/0.980	0.1011/1.013
no. of parameters	293	506	278
R1[a] (F_0), wR2[b] (F_0) ($I \geq 2\sigma(I)$)	0.0464, 0.1165	0.0753, 0.2055	0.0622, 0.1720
CCDC No.	616937	616938	616939

[a] $R = \Sigma||F_o| - |F_c||/\Sigma|F_o|$. [b] $wR = [\Sigma[w((F_o^2 - F_c^2)^2]/[\Sigma w(F_o^2)^2]^{1/2}$.

Scheme 1. Synthetic Strategy for the Preparation of the Unsupported Hydroxo-Bridged Complexes **1**–**3**[a]

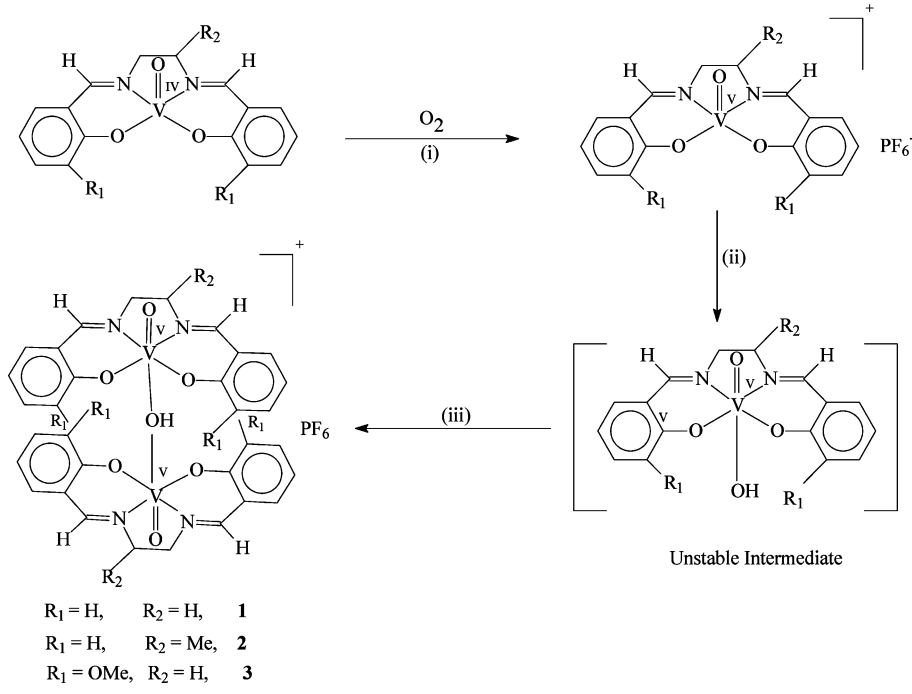

[a] Conditions: (i) NH_4PF_6, THF, reflux, anion-assisted aerial oxidation; (ii) OH^- (presumably from residual moisture in the solvent); (iii) $[VOL^{1-3}]^+PF_6$ (present in the reaction mixture).

more ancillary bridging ligands, connecting a pair or more of the vanadium centers together.[14a–c,e–h,15–17] Excepting a few,[14f,h] all these compounds have been prepared at controlled pH by the addition of acid or base that helped in the generation of the hydroxo group as ligand. The protocol used for the synthesis of **1**–**3**, on the other hand, does not include any deliberate attempt to introduce an OH^- ligand in the reaction medium. $[V^{IV}O(Salen)]$ is known, as discussed in our earlier communication,[13a] to undergo aerial oxidation in solution in the presence of an added anion which is accommodated in the vacant coordination site of vanadium(V), *trans* to the terminal oxo-ligand.[27] This binding is more of an ionic nature as confirmed in solution by NMR study.[27b] We followed the same reaction of $[V^{IV}O(Salen)]$ in the presence of bulky PF_6^- anion. The oxidized $[V^VO(Salen)]^+$ cation fails to accommodate PF_6^- in its vacant coordination site, possibly because of the large size and low surface charge density of the anion. This in turn forces the vanadium(V) center in $[V^VO(Salen)]^+$ to accept a hydroxo

(27) (a) Bonadies, J. A.; Butler, W. M.; Pecoraro, V. L.; Carrano, C. J. *Inorg. Chem.* **1987**, *26*, 1218. (b) Oyaizu, K.; Dewi, E. L.; Tsuchida, E. *Inorg. Chem.* **2003**, *42*, 1070.

group as ligand from the residual moisture present in the solution[14f,h] and to get stabilized through the formation of an unsupported μ-OH bridge between a pair of participating vanadium(V) centers. Of particular interest in the structures of **1**–**3** is the *trans* location of μ-OH group relative to the terminal oxo- ligand (vide infra). All the structurally characterized oxovanadium compounds with bridging or terminal hydroxo ligand(s) on the contrary have a terminal oxo-group, *cis* to the coordinating OH^- ligand.[14–17,26]

Magnetic susceptibility values indicate that all the complexes (**1**–**3**) are diamagnetic in nature. The molar conductivities of these compounds in acetonitrile are in the range 131–143 Ω^{-1} cm^2 mol^{-1} as expected for 1:1 electrolytic behavior.[28]

IR spectra of the complexes are summarized in the Experimental Section, containing all the characteristic bands of the coordinated N_2O_2 ligands. These include prominent bands at about 1626 and 1275 cm^{-1} attributable to the ν(*C*═N) and ν(C—O/phenolate) stretching modes of the ligands. In addition, a sharp strong band is observed attributable to the terminal V═O_t stretching at about 951 cm^{-1}, which is significantly lower in wavenumber than what previously has been reported for the mononuclear [V^{V}O(Salen)]$^+$ entity (981 cm^{-1}).[27a] The results confirm the presence of a bridging moiety *trans* to the terminal oxo-groups in **1**–**3**. Of particular interest here is the appearance of a new signal at about 658 cm^{-1}, considered to be a signature for the antisymmetric ν(V—OH) stretching mode.[26c] Also, the μ-hydroxo-bridge that connects the vanadium centers together provides a moderately strong antisymmetric bridge vibration at about 815 cm^{-1} along with a broadband in the 3422–3446 cm^{-1} region. The strong vibrations observed at about 843 cm^{-1} are characteristic of the PF_6^- counteranion in these compounds.[29]

The cationic complexes in **1**–**3** thus appear to be dinuclear with a 2-fold axis of symmetry and bridged by a uninegative atom or a group of atoms, namely, F^- or OH^-. Leigh et al.[30] have recently reported a single fluoride bridged compound [(Salen)VO(μ-F)OV(Salen)]BF_4 obtained by a closely comparable reaction which involves interaction of [V^{IV}O(Salen)] with HBF_4.Et_2O in acetonitrile. The presence of an F^- ion in the bridging portion has been conclusively established by a ^{19}F NMR study. For compounds **1**–**3**, ^{19}F NMR spectra are all identical (Supporting Information Figure S1) involving a single strong feature in the form of a doublet at −72.2 ppm ($J_{P—F}$ = 751 Hz) due to ^{31}P (I = 1/2) coupling, corresponding to the PF_6^- anion.[31] The lack of a characteristic signal due to the bridging F^- ion (at ca. −136 ppm)[30] in **1**–**3** therefore leaves the OH^- ion as the only viable alternative for the bridging moiety in these compounds.

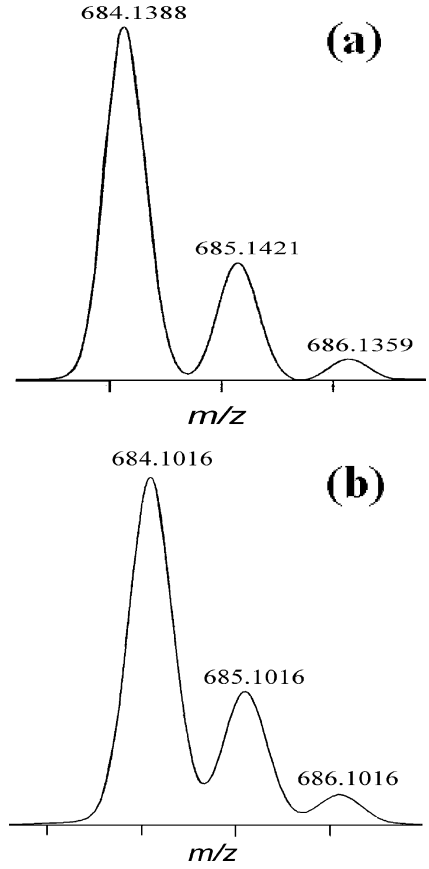

Figure 1. Molecular ion peak in the ESI mass spectrum (positive) for complex **1** in acetonitrile with observed (top, **a**) and simulated (bottom, **b**) isotopic distributions.

^{51}V NMR spectra in acetonitrile-d_3 of **1**–**3** display a single broad signal in the −584 to −564 ppm region (spectral width at half-height, $\Delta\nu_{½}$ varies between 3600 and 2500 Hz) thus fulfilling the symmetry requirement for these molecules.

Mass Spectroscopy. ESI-MS spectral data (in the positive ion mode) for the complexes **1**–**3** are listed in the Experimental Section. All these complexes display their respective molecular ion peak due to the [M-PF_6]$^+$ ionic species ([M-PF_6-2THF]$^+$ in case of **1**). The isotope distribution pattern for the molecular ion peak of **1** is displayed in Figure 1a together with its simulation pattern (Figure 1b). Results confirm the identities of these compounds as containing two identical vanadium(V) centers connected by an unsupported hydroxo-bridge.

Description of Crystal Structures. Perspective views of the molecular structures of **1**–**3** are shown in Figures 2, 3, and Supporting Information Figure S2, respectively. Selected bond distances and angles are summarized in Table 2. The results provide confirmatory evidence in support of their proposed binuclear compositions. Complex **1** crystallizes in the monoclinic space group $P2_1/c$ while **2** crystallizes in the triclinic space group $P\bar{1}$, both having two molecular weight units accommodated in the unit cell. **3** on the other hand, has a tetragonal space group $I4_1/acd$ with sixteen molecular weight units in the unit cell. In **1** are also present two independent THF molecules as solvent of crystallization,

(28) Geary, W. J. *Coord. Chem. Rev.* **1971**, *7*, 81.
(29) Nakamoto, K. *Infrared and Raman Spectra of Inorganic and Coordination Compounds*, 5th Ed.; VCH-Wiley: New York, 1997.
(30) (a) Fairhurst, S. A.; Hughes, D. L.; Leigh, G. J.; Sanders, J. R.; Weisner, J. *J. Chem. Soc., Dalton Trans.* **1994**, 2591. (b) Choudhary, N. F.; Hitchcock, P. B.; Leigh, G. J. *Inorg. Chim. Acta* **2000**, *310*, 10.
(31) (a) Paul, R. L.; Argent, S. P.; Jeffery, J. C.; Harding, L. P.; Lynam, J. M.; Ward, M. D. *J. Chem. Soc., Dalton Trans.* **2004**, 3453. (b) Günther, H. *NMR Spectroscopy*; John Wiley & Sons: Chichester, 1980; p 220.

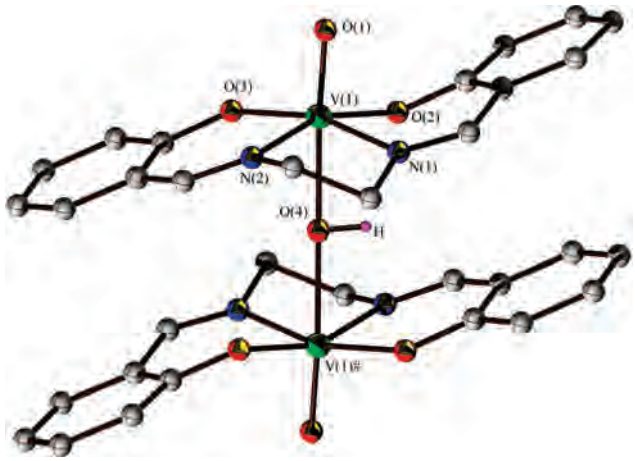

Figure 2. Molecular structure and atom-numbering scheme for **1** with thermal ellipsoids drawn at the 30% probability level. The refined hydrogen atom position of the bridging hydroxide ligand is shown. The V−O(H)−V bridge is in the plane of the paper.

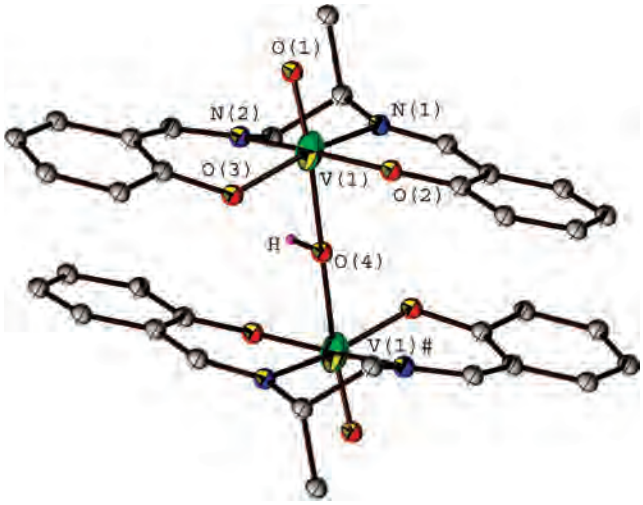

Figure 3. ORTEP view of the hydroxo-bridged cation in **2**, showing the atomic numbering scheme with thermal ellipsoids drawn at the 30% probability level. The H atoms of the two $(L^2)^{2-}$ ligands are omitted for clarity, while that bound to oxygen atom of hydroxo-bridge is depicted as its refined position.

occupying the void volumes. The asymmetric unit of **2** contains two independent molecules (**2A** and **2B**) with only minor conformational differences between these as summarized in Supporting Information Table S1. For the sake of brevity, in the remaining part of this discussion, only the salient features of **2A** will be discussed along with **1** and **3**.

All the reported compounds have the PF_6^- as counterion. The cationic parts are all centrosymmetric involving two $[V^VOL]^+$ units (H_2L = H_2L^1−H_2L^3)[20] connected together by an oxygen atom O(4) from the bridging hydroxo moiety, thus forming a hither to unknown linear V(V)—(*μ*-OH)—V(V) core.

Each vanadium(V) center in these molecules has a distorted octahedral geometry. The basal positions are occupied by the donor atoms O(2), O(3), N(1), and N(2), all contributed by the tetradentate ligand $(L)^{2-}$ (Salen and its derivatives). The apical positions are taken up by the terminal oxygen atom O(1), together with the bridging oxygen atom O(4). In **1**, the *trans* angles in the basal plane

Table 2. Selected Bond Distances (Å) and Angles (deg) for the Complexes **1**, **2**, and **3**

	1	**2A**	**3**
	Bond Distances (Å)		
V(1)—O(1)	1.609(2)	1.570(5)	1.598(2)
V(1)—O(2)	1.833(2)	1.812(4)	1.834(2)
V(1)—O(3)	1.8233(18)	1.842(5)	1.836(2)
V(1)—O(4)	2.0655(2)	2.0552(12)	2.0533(6)
V(1)—N(1)	2.061(2)	2.101(5)	2.098(3)
V(1)—N(2)	2.085(2)	2.074(5)	2.071(3)
O(4)-H	0.884(10)	0.901(12)	0.888(10)
V(1)···V(1)#	4.131	4.110	4.107
	Bond Angles (deg)		
O(1)—V(1)—O(2)	97.44(10)	100.6(3)	100.41(12)
O(1)—V(1)—O(3)	100.70(10)	97.3(3)	97.43(11)
O(1)—V(1)—O(4)	172.28(7)	172.37(19)	172.82(10)
O(1)—V(1)—N(1)	91.10(9)	98.7(3)	96.91(12)
O(1)—V(1)—N(2)	96.85(10)	90.4(2)	89.85(13)
O(4)—V(1)—N(1)	81.48(6)	79.37(17)	80.50(8)
O(4)—V(1)—N(2)	79.51(7)	81.97(16)	83.04(8)
O(4)—V(1)—O(2)	84.31(6)	86.69(17)	86.13(8)
O(4)—V(1)—O(3)	85.95(7)	82.39(15)	83.13(7)
O(2)—V(1)—O(3)	106.20(9)	108.11(19)	108.81(10)
O(2)—V(1)—N(1)	86.78(9)	86.4(2)	85.67(11)
O(2)—V(1)—N(2)	158.63(9)	160.2(2)	160.58(11)
O(3)—V(1)—N(2)	86.60(9)	86.4(2)	85.88(11)
O(3)—V(1)—N(1)	160.97(9)	155.9(2)	157.33(11)
N(1)—V(1)—N(2)	77.13(9)	75.6(2)	76.69(12)
V(1)—O(4)—H	90.01(4)	90.4(6)	90.5(6)
V(1)—O(4)—V(1)#	180.00(2)	180.00(8)	180.00(4)

Table 3. Bond Valence Sum[a] for the Oxygen Atom O(4) of the Bridging Hydroxo Group in **1**–**3**

compound[b]	bond description	r_{ij}, Å	s_{ij}	$V_{ij} = \Sigma_j s_{ij}$
1	O(4)−V(1)	2.0655	0.492	
	O(4)−V(1)#	2.0655	0.492	0.984
2	O(4)−V(1)	2.0552	0.506	
	O(4)−V(1)#	2.0552	0.506	1.012
3	O(4)−V(1)	2.0533	0.508	
	O(4)−V(1)#	2.0533	0.508	1.016

[a] r_0 = 1.803 Å; B = 0.37. [b] The independent molecule **2A** has been taken from the asymmetric unit of **2**.

O(2)—V(1)—N(2) 158.63(9)° (corresponding angles in **2A** and **3** are 160.2(2)° and 160.58(11)°, respectively) and O(3)—V(1)—N(1) 160.97(9)° (155.9(2)° and 157.33(11)°) are somewhat compressed and force the V(1) atom by 0.2309 Å (0.2401 and 0.2235 Å) out of the least-squares basal plane toward the more tightly held apical oxo- atom O(1). The distances and angles made by the donor atoms in the equatorial plane at V(1) (Table 2) are in the expected range as previously reported for compounds containing the $[V^VO(Salen)]^+$ moiety.[27,30] These basal planes surrounding the two vanadium(V) centers are almost parallel with a staggered conformation as judged by the near zero value of the dihedral angle between them.

In the linear V(V)—(*μ*-OH)—V(V) core of **1**–**3**, the oxygen atom O(4) is situated at the center of inversion. Of particular interest here is the *trans* location of the bridging hydroxo moiety relative to the terminal oxygen atom O(1), such that the angle O(1)—V(1)—O(4) 172.28(7)° (172.37(19)° and 172.82(10)°) is close to linearity, as expected for a nearly ideal octahedral geometry. This leads to a significant increase in the V(1)—O(4) distance, 2.0655(2) Å (2.0552(12) and 2.0533(6) Å) attributable to the *trans* labilizing influence of the terminal oxo- atom O(1). In consequence, the enlarged

V(1)···V(1)# separation 4.131 Å (4.110 and 4.107 Å) is by far the largest in these compounds compared with the other divanadium(V, IV, and III) compounds containing one or more hydroxo group(s) as bridging ligands.[14–17] The terminal V(1)—O(1) distance 1.609(2) Å (1.570(5) and 1.598(2) Å) is a little longer compared with those (1.576 Å)[27] in $[V^{V}O(Salen)ClO_4]$ and $[V^{V}O(Salen)BF_4]$, indicating stronger interactions from the OH^- ligand compared to those from its ClO_4^- and BF_4^- analogues.

The torsion angle O(1)—V(1)···V(1)#—O(1)# is exactly 180° in **1**–**3**, making the $[V_2O_2(OH)]^{5+}$ core perfectly linear in these compounds. To our knowledge, such linearity is an unprecedented structural feature in divanadium compounds.

Bond Valence Sum (BVS) Approach. The bond length ($r_{i,j}$) between the two participating atoms (i, j) is related to the bond valence (s_{ij}) by eq 1 where r_0 and B are

$$s_{ij} = \exp[(r_0 - r)/B] \quad (1)$$

two empirically determined parameters, the former being the characteristic of a bond in question.[32] For a multiatomic system containing a central atom, the bond valence s_{ij} may be regarded as the amount of electrons by which the central atom (i) is enriched (or depleted) in forming a bond with a neighboring atom (j). Accordingly, the BVS (V_i) of an atom in question is a measure of the total number of electrons it uses to form the compound (i.e., oxidation state) and is calculated by eq 2. As long as the bond

$$V_i = \sum s_{ij} \quad (2)$$

lengths are all controlled by electronic factors in a particular compound, BVS provides an excellent fit to the observed oxidation state. However, in molecules having steric encumbrances where nonelectronic factors (steric, etc.) have dominant role(s) to play in controlling bond lengths, the BVS value cannot be used as a measure of the formal oxidation state unless the steric feature is constant.[33] Brown and Altermatt[34] have calculated the r_0 value for the $V^{5+}-O^{2-}$ bond to be 1.803 Å, with the empirical parameter B being set to 0.37. Substituting these numbers in eqs 1 and 2, the bond valence contributions of the attached vanadium center to the bridging oxygen atom O(4) have been calculated for **1**–**3**. As summarized in Table 3, the data indicate one unit of V_i being contributed to the bridging oxygen atom O(4) by the attached vanadium centers V(1) and V(1)#. The results thus provide a strong evidence in favor of O(4) being a part of a bridging hydroxo moiety. The hydrogen atom of that moiety consumes the remaining unit of V_i with the central oxygen atom.

^{1}H NMR Spectroscopy. ^{1}H NMR spectra of **1**–**3** have been recorded at room temperature in acetonotrile-d_3, and the data are summarized in Table 4. The complexes, as expected, do not display any low field resonance beyond 8.40 ppm, thus indicating the absence of phenolic-OH protons of the free tetradentate ligands, $H_2L^1-H_2L^3$. The spectra of **1**, **2**, and **3** are displayed in Figures 4, and 5, and Supporting Information Figure S3, respectively, along with their possible interpretations.

Table 4. ^{1}H NMR Data (δ, ppm)[a] for the Complexes **1**–**3** in Acetonitrile-d_3

1		**2**		**3**		assignments
8.26 s	4H	8.42–8.06 s	4H	8.26 s	4H	H(7), H(7′)
7.23 (7.28) d	4H	7.80–6.68 m	16H	7.13 (6.56) d	4H	H(5), H(5′)
7.60 (7.13) t	4H			6.97–6.89 m	8H	H(4), H(4′)
6.92 (8.23) t	4H					H(3), H(3′)
6.78 (8.05) d	4H					H(2)[b], H(2′)[b]
4.06, 3.90 (5.03) q	8H	4.19–3.80 m	6H	4.07, 3.80 brd	8H	H(8), H(8′)
		1.29 (5.83) d	6H			H(9)[c]
				3.88 s	12H	H(10)[d], H(10′)[d]

[a] Chemical shifts (δ) relative to internal TMS at room temperature. Protons labels are as in the insets in Figures 4 and 5 and Supporting Information Figure S3. s, singlet; d, doublet; t, triplet; brd, broad doublet; q, AB quartet. Values in parentheses represent coupling constants (J in Hz). [b] H(2) protons are absent in **3**. [c] H(9) protons are present only in **2**. [d] H(10) protons are present only in **3**.

For compounds **1** and **3**, their spectral features have very much in common, both involving a singlet (appearing at 8.26 ppm) corresponding to the presence of the azomethine moiety and a broad doublet due to the bridge-head ethylene protons. The latter protons H(8) and H(8′) are diastereotopic in these complexes because of the rigidity of the metal-bound bridge-head moiety in the coordinated ligands and appear as an AB spin system with $\delta_A = 4.06$ and $\delta_B = 3.90$ ppm in **1**. A sharp singlet at 3.88 ppm is characteristic of the OMe protons in **3**. All the aromatic protons in **1** appear in the 7.62–6.76 ppm region with the expected splitting and integration patterns.

Because of the presence of two chiral centers in **2**, the spectral features of this compound (Figure 5) is a bit more complicated but at the same time quite interesting. Thus, the azomethine protons H(7), which appear as a singlet in **1**, are split into four lines of equal intensity in the 8.4–8.0 ppm region. With a couple of methyl groups attached to the anisochronous bridge-head carbon atoms C(8) and C(8)#, two diastereomeric pairs of enantiomers (RR/SS and RS/SR) are possible for this compound, and for each pair, two azomethine signals are expected because of the inequivalence of the H(7) and H(7′) protons. The appearance of four signals of equal intensities (shown in the inset) thus indicates the presence of both the diastereomeric pairs to form a racemic mixture. Interestingly, these singlets gradually lose their integrity with the rise in temperature and eventually coalesce partially into a pair of broad signals at 70 °C (Figure 6). This change, as expected, is reversible and points to an equilibrium between these two diastereomeric pairs. The aromatic protons in **2**, all appear in the form of complex multiplets in the 7.80–6.68 ppm range as against a couple of doublets and triplets observed for **1**. The bridge-head aliphatic protons H(8) and H(8′) appear as a cluster of three signals in the 4.19–3.80 ppm region. The methyl protons H(9), which emerge as a twin signal at 1.29 ppm near room temperature, show up as a pseudo triplet (consisting of two overlapping doublets) at 0 °C, as expected for the diastereomeric forms. Unfortunately, we are unable to detect any signal corresponding

(32) (a) Brown, I. D. *Chem. Soc. Rev.* **1978**, *7*, 359. (b) Brown, I. D. *Acta Crystallogr.* **1992**, *48B*, 553.
(33) Whangbo, M.-H.; Torardi, C. C. *Science* **1990**, *249*, 1143.
(34) Brown, I. D.; Altermatt, D. *Acta Crystallogr.* **1985**, *41B*, 244.

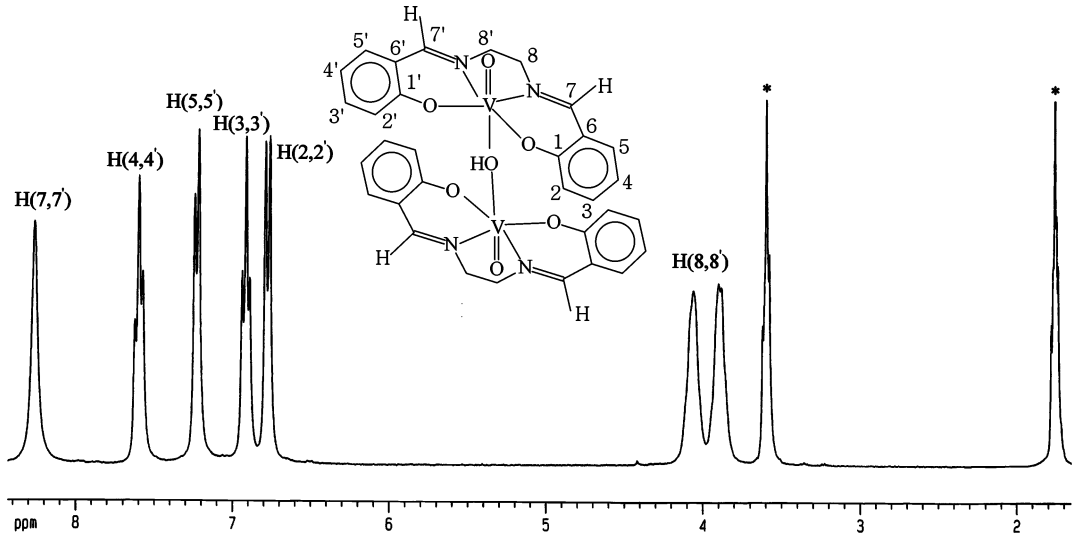

Figure 4. 300 MHz ^{1}H NMR spectrum of compound **1** in acetonitrile-d_3 at 293 K. The peaks marked with asterisk denote solvent impurities.

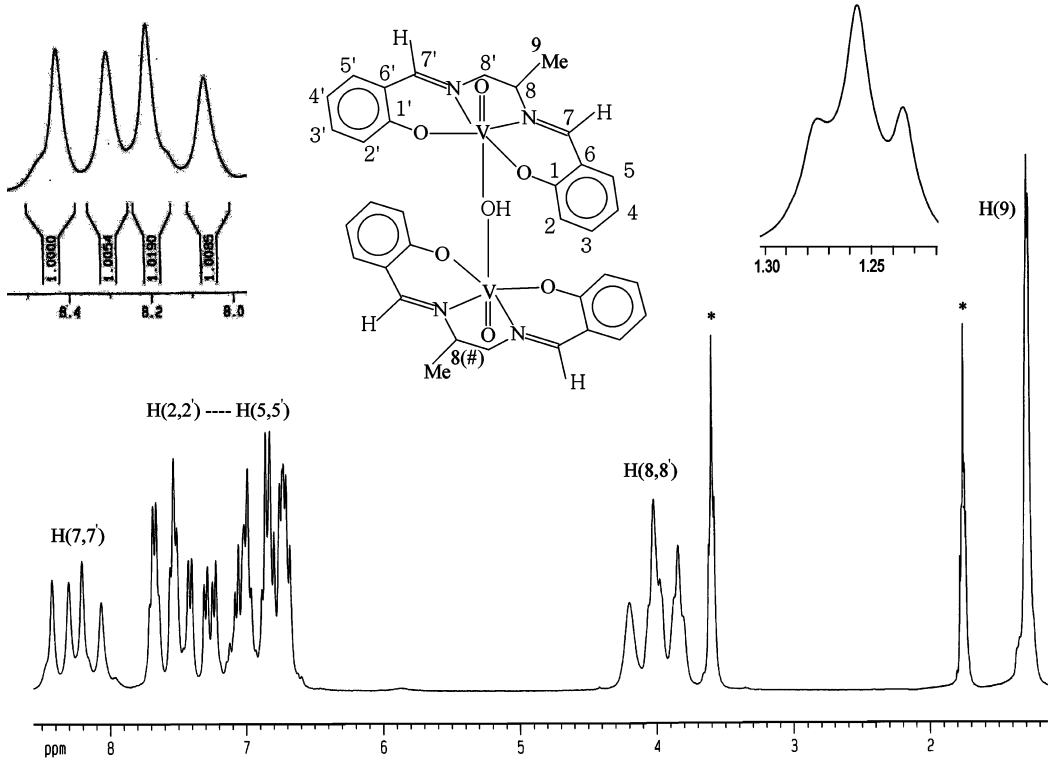

Figure 5. ^{1}H NMR spectrum of compound **2** in acetonitrile-d_3 at room temperature. The insets show azomethine and methyl signals in magnified forms. The peaks marked with an asterisk denote solvent impurities.

to the bridging hydroxo moiety in these compounds. The results, however, have conclusively established the retention of the dimeric structures in solution for **1**–**3**.

Electronic Spectroscopy. Electronic absorption spectra of the complexes **1**–**3** have been recorded in acetonitrile, and the relevant data are summarized in the Experimental Section. A representative spectrum of **3** is displayed in the Supporting Information Figure S4. All these complexes display two prominent absorptions, one in the visible region (575–640 nm) in the form of a medium intensity (ε, 2100–2400 mol^{-1} cm^2) band whose position appears to be sensitive to the substituent present in the phenyl ring. We interpret this band as arising from a ligand-to-metal charge-transfer (LMCT, PhO$^-$ → V (dπ)). The second one in the near-UV region (320–355 nm), appearing as a shoulder with much stronger intensity (ε, *ca.* 17 000 mol^{-1} cm^2), also has a charge-transfer (OH$^-$ → V) origin.[7d,35] The remaining band maxima in the UV region are attributable to ligand internal transitions.

Electrochemistry. The electrochemical behavior of **1**–**3** has been examined by cyclic voltammetry (CV) in acetonitrile (0.1 M TBAP) using a platinum working electrode. A potential window of −2.0 to +2.0 V versus Ag/AgCl reference has been chosen in which the ligands are electrode inactive. The voltammetric features are roughly identical for

(35) Patra, A. K.; Ray, M.; Mukherjee, R. *Polyhedron* **2000**, *19*, 1423.

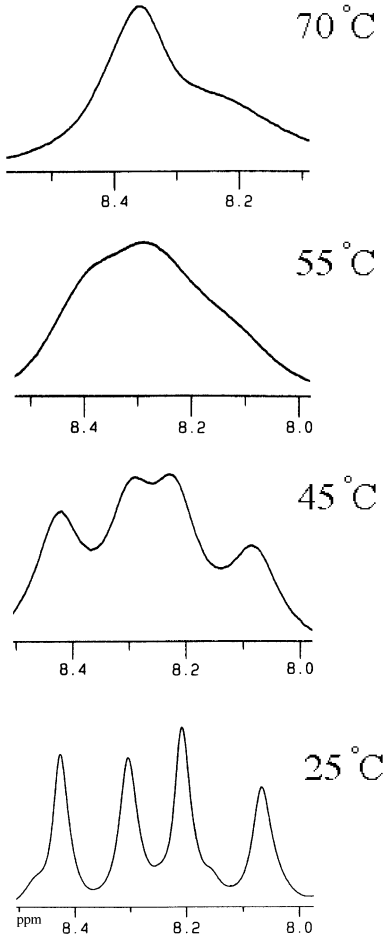

Figure 6. Variable temperature ^{1}H NMR spectra of **2** in acetonitrile-d_3 solution, showing a gradual coalescence of the signals due to azomethine protons with the rise in temperature.

these compounds as summarized in Table 5. Both CV and normal pulse voltammogram (NPV) of **1** in the potential range from −0.4 to +0.8 V are displayed in Figure 7 as a representative example. The voltammograms include three electrochemical responses at $(E_{1/2})_{\mathrm{I}} = 0.57$ V (process I), $(E_{1/2})_{\mathrm{II}} = 0.39$ V (process II), and $(E_{1/2})_{\mathrm{III}} = 0.04$ V (process III). On the basis of a comparison with the ferrocenium/ferrocene couple (ΔE_p, 70 mV at 100 mVs^{-1}), processes I and III may be appropriately described as reversible,[36] both involving a single electron (ΔE_p, 60 and 74 mV at 100 mVs^{-1} for processes I and III, respectively).

All the three processes are cathodic as judged by the steady state voltammetry (using an ultramicro platinum electrode, 10 μM diameter). Electron stoichiometry determination for these processes by constant potential coulommetry, unfortunately, proved unsuccessful because of the continuous coulomb accumulation due to unidentified electrode reaction(s) in the larger time-scale of the experiment. However, a comparison of the wave heights in the adjoining NPV (Figure 7) indicates that processes I and III have identical electron stoichiometry while process II involves twice as many numbers of electrons.

(36) Brown, E. R.; Large, R. F. *Electrochemical Methods. In Physical Methods in Chemistry*; Weissberger, A., Rossiter, B., Eds.; Wiley-Interscience: New York, 1971; Part IIA, Chapter VI.

The electrochemical behavior of [VO(Salen)] is well documented.[27,37] It undergoes a reversible one electron oxidation at 0.54 V attributable to V(IV)/V(V) electron-transfer. Taking a cue from these studies, one can describe process I as arising from a V(V)−V(V)/V(V)−V(IV) electron-transfer, generating a V(V/IV) mixed-oxidation product. Process II on the other hand appears to be a single-step two-electron process as indicated by both NPV and differential pulse voltammetric (DPV) experiments (shown in Figure 7, inset), comprising a V(V)−V(IV)/V(III)−V(IV) redox couple. Finally, for process III, an isovalent divanadium(III) species is conjectured to be the product of the electrode reaction through a V(III)−V(IV)/V(III)−V(III) electron-transfer.[26c,38] Interestingly, process III fails to appear in the voltammogram of **3**. We believe that the electron donating OCH_3 groups in the ligand aromatic rings of **3** make the coordinated vanadium center richer in electron density, and that probably resists the incoming electron needed for this reduction process.

In summary, the electrochemical results (combined with NPV and DPV) thus indicate the possible involvements of four binuclear vanadium species with oxidation state combinations shown by eqs 3–5.

$$[(\mathrm{L})\mathrm{OV^{V}}(\mu\text{-}\mathrm{OH})\mathrm{V^{V}O(L)}]^{1+} \underset{(E_{1/2})_{\mathrm{I}}=0.57\ \mathrm{V}}{\overset{\text{Process I}\ +e^-}{\rightleftharpoons}} [(\mathrm{L})\mathrm{OV^{V}}(\mu\text{-}\mathrm{OH})\mathrm{V^{IV}O(L)}]^{0} \quad (3)$$

$$[(\mathrm{L})\mathrm{OV^{V}}(\mu\text{-}\mathrm{OH})\mathrm{V^{IV}O(L)}]^{0} \underset{(E_{1/2})_{\mathrm{II}}=0.39\ \mathrm{V}}{\overset{\text{Process II}\ +2e^-}{\rightleftharpoons}} [(\mathrm{L})\mathrm{OV^{III}}(\mu\text{-}\mathrm{OH})\mathrm{V^{IV}O(L)}]^{2-} \quad (4)$$

$$[(\mathrm{L})\mathrm{OV^{III}}(\mu\text{-}\mathrm{OH})\mathrm{V^{IV}O(L)}]^{2-} \underset{(E_{1/2})_{\mathrm{II}}=0.04\ \mathrm{V}}{\overset{\text{Process III}\ +e^-}{\rightleftharpoons}} [(\mathrm{L})\mathrm{OV^{III}}(\mu\text{-}\mathrm{OH})\mathrm{V^{III}O(L)}]^{3-} \quad (5)$$

In the cathodic range, **1**–**3** also display an irreversible process at about −1.6 V (process IV). A similar irreversible electrode process is known to appear in the voltammogram of [VO(Salen)][37] and is tentatively explained as attributable to the elimination of a terminal oxygen from the vanadium center. Further discussion on this process is beyond the scope of this investigation.

Concluding Remarks

A series of divanadium(V) compounds (**1**–**3**) bridged by an unsupported hydroxo-group has been reported for the first time. The bridging group is situated *trans* to the terminal oxo-group. In consequence, the separations between the two participating vanadium centers V(1)···V(1)# in these com-

(37) (a) Kapturkiewicz, A. *Inorg. Chim. Acta* **1981**, *53*, L77. (b) Seangprasertkij, R.; Riechel, T. L. *Inorg. Chem.* **1986**, *25*, 3121. (c) Tsuchida, E.; Yamamoto, K.; Oyaizu, K.; Iwasaki, N.; Anson, F. C. *Inorg. Chem.* **1994**, *33*, 1056;. and references cited therein.

(38) (a) Bonadies, J. A.; Pecoraro, V. L.; Carrano, C. J. *J. Chem. Soc., Chem. Commun.* **1986**, 1218. (b) Köppen, M.; Fresen, G.; Wieghardt, K.; Llusar, R. M.; Nuber, B.; Weiss, J. *Inorg. Chem.* **1988**, *27*, 721. (c) Knopp, P.; Wieghardt, K. *Inorg. Chem.* **1991**, *30*, 4061.

Table 5. Summary of Electrochemical Data[a]

	process I		process II		process III		process IV
compound	$(E_{1/2}{}^{b})_{I}$, V	$\Delta E_p{}^{c}$, mV	$(E_{1/2}{}^{b})_{II}$, V	$\Delta E_p{}^{c}$, mV	$(E_{1/2}{}^{b})_{III}$, V	$\Delta E_p{}^{c}$, mV	E_{pc}, V
1	0.57	60	0.39	65	0.04	74	−1.55
2	0.55	48	0.36	80	0.04	60	−1.60
3	0.53	41	0.34	71			−1.57

[a] Solvent, acetonitrile; supporting electrolyte, TBAP (0.1 M); solute concentration, about 10^{-3} M; working electrode, platinum; temperature, 25 °C. All potentials are vs Ag/AgCl reference, estimated by cyclic voltammetry at a scan rate of 100 mV s^{-1}. [b] $E_{1/2} = 0.5(E_{pc} + E_{pa})$. [c] $\Delta E_p = E_{pc} - E_{pa}$.

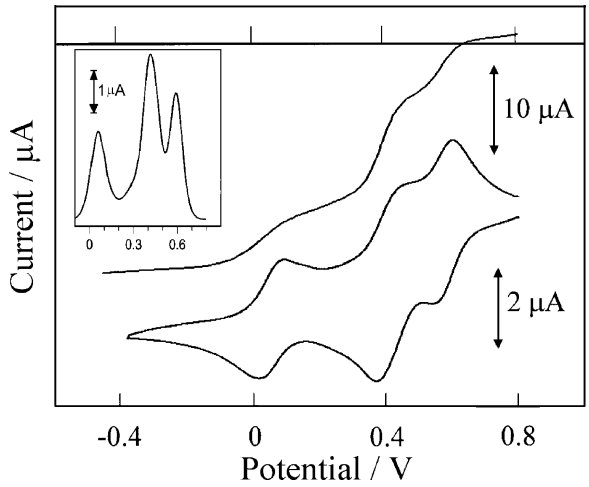

Figure 7. Cyclic and normal pulse voltammograms of **1** in acetonitrile solution; potentials vs Ag/AgCl, 0.1 M TBAP at a platinum electrode, scan rate 100 mVs^{-1}. The inset shows the differential pulse voltammogram establishing the single-step two-electron involvement in process II.

pounds are by far the largest (ca. 4.131 Å) compared with any other divanadium(V, IV, and III) compounds containing one or more hydroxo group(s) as bridging ligands.[14–17] These compounds also retain their identity in solution (in dry organic solvents) as confirmed by ^{1}H NMR spectroscopy. Electrochemically also, **1**–**3** are quite interesting, undergoing three (two for **3**) nearly reversible metal-centered electron transfers, all in the positive potential range (vs Ag/AgCl). One of these is a single-step two-electron transfer as indicated by normal and differential pulse voltammetries.

Acknowledgment. This work was supported by the Council of Scientific and Industrial Research (CSIR), New Delhi. Three of us (P.B.C., D.M., and A.A.) also thank the CSIR for the award of Research Fellowships. M.C. thanks the authorities of Sophia University, Japan for a Lecturing-Research Grant, 2006.

Supporting Information Available: ^{19}F NMR spectra of **1** and **2**, ORTEP diagram, ^{1}H NMR and electronic absorption spectrum of **3** (Figures S1–S4), selected bond distances and bond angles for the independent molecule **2B** (Table S1, PDF), and X-ray crystallographic files in CIF format for the compounds **1**–**3**. This material is available free of charge via the Internet at http://pubs.acs.org.

IC702286H